On the Possibility of Real-Time Monitoring of Glucose in Cell Culture by Microdialysis Using a Fluorescent Glucose Binding Protein Sensor

Xudong Ge, Govind Rao, and Leah Tolosa*

Center for Advanced Sensor Technology, Department of Chemical and Biochemical Engineering, University of Maryland Baltimore County, 1000 Hilltop Circle, Baltimore, Maryland 21250

Although glucose sensors with millimolar sensitivity are still the norm, there is now a developing interest in glucose sensors with micromolar sensitivity for applications in minimally invasive sampling techniques such as fast microdialysis and extraction of interstitial fluid by iontophoresis and laser poration. In this regard, the glucose binding protein (GBP) with a binding constant for glucose in the micromolar range is of particular relevance. GBP is one of the soluble binding proteins found in the periplasmic space of Gram-negative bacteria. Because of its hinge-like tertiary structure, glucose binding induces a large conformational change, which can be used for glucose sensing by attaching a polarity sensitive fluorescent probe to a site on the protein that is allosterically responsive to glucose binding. Correspondingly, the resulting optical biosensor has micromolar sensitivity to glucose. Because binding is reversible, the biosensor is reusable and can be stored at 4 °C for 6 months without losing its sensitivity. In this paper, we show the feasibility of using the GBP biosensor to monitor glucose in microdialysis. The effect of perfusion rate, bulk glucose concentration and temperature on microdialysis efficiency was determined. Additionally, the glucose concentrations in mammalian cell culture were monitored to demonstrate the applicability of this sensor in complex and dynamic processes over a period of time. As the sensor is sensitive to micromolar glucose, high dialysis efficiency is not required when the bulk glucose concentration is within the millimolar physiological range. Thus, a perfusion rate of 10 μL/min or faster can be used, resulting in delay times of 1 min or less.

Introduction

Glucose monitoring is very important in bioprocesses such as fermentation and mammalian cell culture. As glucose is the major energy source for cells, optimal glucose concentrations are crucial in healthy cell growth and efficient product yield. In addition, glucose analysis is of importance as a clinical indicator of diabetes. Because the glucose concentration in cell culture media and human blood is in the millimolar range, currently available glucose sensors predictably have millimolar sensitivities. Most of these glucose sensors utilize glucose oxidase as the biological element. In this design, the enzyme is immobilized in a polymer or a porous membrane (*1*−*11*) in close contact with a polarized electrode. When exposed to glucose, the enzyme converts glucose into gluconolactone and hydrogen peroxide, which is then detected by the electrode. Another protein that has been investigated as a possible glucose sensor is concanavalin A (*12*−*15*). This sensor utilizes the competition between glucose and a sugar-containing macromolecule like dextran for binding to the ConA. In addition, D'Auria et al. used coenzyme-depleted enzymes labeled with ANS as the signal transducers (*16*−*18*).

With advancements in diabetes research, it became apparent that continuous monitoring of blood glucose levels is far superior to the intermittent testing from finger pricks that is now accepted practice. Additionally, relatively painless and minimally invasive sampling promotes patient compliance. Thus, novel sampling techniques such as fast microdialysis (*19*), extraction of interstitial fluid by iontophoresis (*20*) and laser poration (*21*, *22*) have emerged in recent years. However, these technologies have inherent barriers that do not allow full extraction of glucose from blood and tissue. For example, to achieve millimolar concentrations of glucose in microdialysis, the dimensions of the probe should be large, which may not be practical for a subcutaneous device. Alternatively, the perfusion rate should be slow which can result in a long lag time. In iontophoresis, the skin itself acts as a barrier when the weak electromotive force is applied to extract glucose from the interstitial fluid. Consequently, it has become necessary to develop new glucose sensors with submillimolar glucose sensitivities.

In the search for glucose sensors with submillimolar sensitivities, ligand-specific periplasmic binding proteins have drawn much attention (*23*−*38*). These binding proteins have a two-domain structure connected by a hinge (*39*). The binding of the ligand at the binding site close to the hinge can induce a large conformational change from an "open" ligand-free structure to a "closed" ligand-bound structure (*40*, *41*). By introducing a polarity-sensitive fluorophore into such a protein, the conformational change in response to ligand binding can be indirectly detected. The result is an optical biosensor that responds in submillimolar concentrations of the ligand (*42*). Many of the papers on the binding proteins have focused on the construction of the biosensors such as the introduction of the mutation, the expression and purification of the protein and labeling of the protein with fluorescent probes. Little has been written on the useful characteristics of such sensors and none on their application in conjunction with novel sampling techniques.

* To whom correspondence should be addressed. Tel: 410-455-3432. Fax: 410-455-6500. E-mail: leah@umbc.edu.

10.1021/bp070411k CCC: $40.75
Published on Web 04/19/2008

The construction and fluorescent labeling of this biosensor has been described previously (*36*, *37*). Monitoring of glucose consumption in cell culture and fermentation through direct assay of the media was shown to be feasible in both large (hundreds of mL) and small (hundreds of μL) culture volumes (*34*). The small cultures in particular are impossible to monitor for glucose concentration using the gold standard glucose oxidase electrodes. We have shown that the micromolar sensitivity and submicromolar limit of detection of the GBP biosensor allowed for dilution of minute volumes of the cell culture media to within the analytical range of GBP. On the basis of this result, we concluded that any sampling technique that inherently dilutes the sample from millimolar to micromolar glucose will work appropriately with the sensor. In this paper, the characteristics of the GBP-based glucose biosensor and its application in fast microdialysis for bioprocess monitoring are investigated. The sensor characteristics including sensitivity, stability, accuracy, reversibility, selectivity and temperature sensitivity were scrutinized further. Additionally, the effects of bulk glucose in the media, perfusion flow rates and temperature on dialysis efficiency were studied.

Materials and Methods

Materials. 6-Acryloyl-2-dimethylaminonaphthalene (acrylodan) and tris(2-carboxyethyl) phosphine (TCEP) were purchased from Invitrogen. Fructose, fucose, galactose, glucose, maltose, mannose, sucrose, DEAE Sephadex A-50, *N*,*N*-dimethylformamide (DMF), NaCl, KH_2PO_4, Na_2HPO_4, NaH_2PO_4, and $MgCl_2$ were purchased from Sigma-Aldrich (St. Louis, MO). Tryptone and yeast extract were obtained from Becton Dickinson (Sparks, MD). All chemicals were used without further purification. Snakeskin pleated dialysis tubing (10 K MWCO) was purchased from PIERCE (Rockford, IL).

GBP Expression, Purification and Fluorophore Coupling. The preparation of the engineered protein and the labeling of the fluorescent probe have been described previously (*30*, *34*−*37*). The plasmid expressing the wild-type GBP was constructed by cloning the *E. coli* K12 MglB gene into vector pTZ18U. The single-cysteine mutation at position 255 was introduced by using the Quick-Change mutagenesis kit from Stratagene (Cedar Creek, TX). The mutated plasmid was then transformed into *E. coli* NM303. The protein was overexpressed by growing the cells in LB media overnight. The cells were then collected by centrifugation and the periplasmic binding protein was released by osmotic shock method (*23*). After the protein was purified on a DEAE Sephadex A-50 column, the protein was labeled with acrylodan by reacting with 10- to 20-fold dye at pH 7.5 for 2 h at room temperature or overnight at 4 °C in the presence of 10-fold TCEP. Unreacted acrylodan was removed by passing through a Sephadex G-25 column. The total protein concentration was determined and the labeling efficiency was estimated from the total protein concentration and the concentration of protein-bound probe, which was calculated from its absorbance and extinction coefficient (*43*). The final product was 0.2 μm filter-sterilized. The filtered protein can be stored at 4 °C for over 6 months without losing its sensitivity (*34*).

Experimental Setup. The experimental setup for microdialysis of buffer solutions and mammalian cell culture is shown in Figure 1. The minibioreactor was produced by Fluorometrix (Stowe, MA). The bioreactor has a volume of 40 mL and has disposable pH and oxygen-sensing patches attached to the bottom for pH and dissolved oxygen monitoring (*44*). It is capable of temperature control. The agitation speed can be adjusted smoothly from 0 to 1000 rpm. The microinjector and

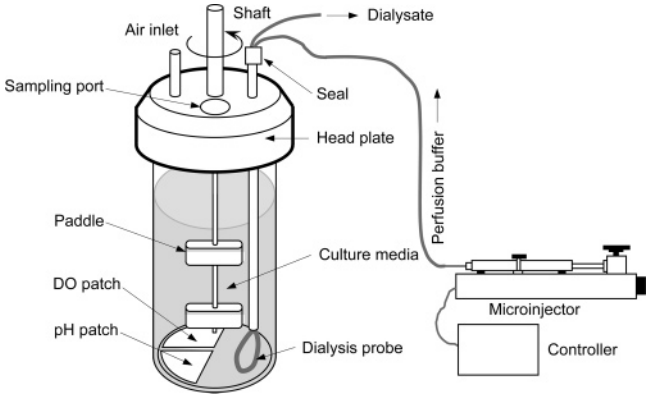

Figure 1. Experimental setup for mammalian cell culture and microdialysis.

controller (Bioanalytical Systems, West Lafayette, IN) is connected through plastic tubing to the dialysis probe (MWCO 10 000), which is immersed in the buffer solution or cell medium. The glucose concentration in the dialysate and the dialysis efficiency were determined as a function of the glucose concentration in the medium, the flowrate of the perfusion buffer, and temperature. In the buffer experiments, the flowrate was adjusted stepwise from 0.1 to 100 μL/min.

Mammalian Cell Culture. A SP2/0 based myeloma/mouse hybridoma cell line (2055.5) secreting an IgG3 antibody specific for the *Neisseria meningitides* capsular-polysaccharide (MCPS) (Rubinstein and Stein, 1988) was maintained in a 250-mL spinner flask (Kontes, Vineland, NJ) in CD Hybridoma protein-free media (Gibco Brand, Carlsbad, CA) supplemented with 2 mM glutamine (HyClone, Laboratories Inc., Logan, UT), 100 U/mL penicillin (HyClone), 100 g/mL streptomycin (HyClone), 1 g/L PF-68 (MP Biomedicals, LLC, Aurora, OH), and 3.5×10^{-4}% mercaptoethanol (v/v) (Sigma, St. Louis, MO). The flask was kept in a water-jacketed incubator (Napco, Winchester, VA). Before performing the cell culture in the bioreactor (Figure 1), the air inlet was covered with a 0.22 μm syringe filter (Millex-GV, Millipore, Bedford, MA). The bioreactor except the dialysis probe, which was ethanol sterilized separately, was then steam sterilized at 121 °C for 25 min. Upon cooling, the vessel was first rinsed with media and then filled with 35 mL of cell culture media inoculated with 7.2×10^4 cells/mL in a laminar flow hood. The process was monitored by DO and pH sensors. The temperature and agitation speed was controlled at 37 °C and 100 rpm. The vessel headspace was open to the atmosphere via the 0.22 μm syringe filter. Dialysate samples were taken twice a day for glucose measurement using a 10 μL/min perfusion rate. Culture samples were withdrawn twice a day with syringes through the sampling port on the vessel for cell counting. Cells in the samples were counted using a hemocytometer.

Fluorescence Measurements. The fluorescence intensity of the labeled protein was measured either in cuvettes on Varian Cary Eclipse fluorescence spectrophotometer (Varian Instruments, Walnut Creek, CA) or in 96-well plates on a SpectraMax M5 plate reader (Molecular Devices, Sunnyvale, CA). To measure the fluorescence intensity in cuvettes, 200 μL of GBP solution was added to a 1.5-mL poly(methylmethacrylate) cuvette (BrandTech Scientific, Essex, CT). After the intensity was measured 10 times, 2.0 μL of glucose standard or sample was added. The mixture was gently vortexed for 10 s, and the intensity was measured again 10 times. The assay was performed in triplicate for each standard or sample. All measurements were made at the same instrumental conditions: excitation wavelength

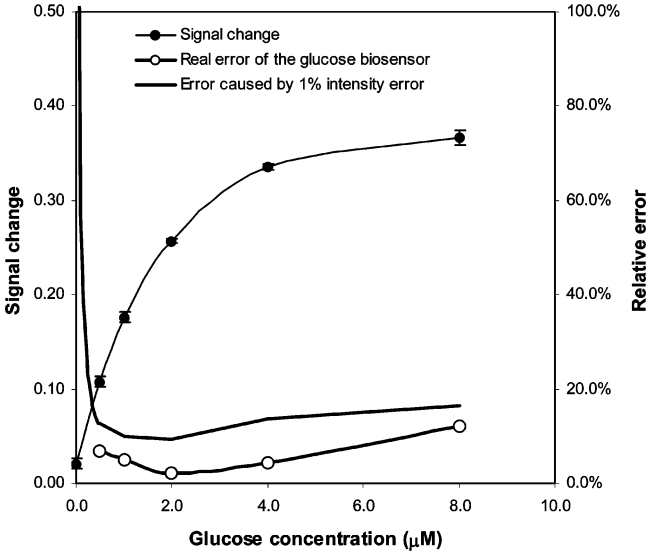

Figure 2. Typical calibration curve and relative measurement error.

380 nm, emission wavelength 510 nm, excitation slit width 5 nm, emission slit width 5 nm, PMT detector voltage 750 V, and average time 0.1 s. To measure the fluorescence intensity in 96-well plates, 200 μL of GBP solution was added to each of the designated wells, and the fluorescence intensities were measured 3 times. Volumes of 2.0 μL of glucose standard or sample were then added to each of the wells. The plate was gently shaken for 10 s, and the intensities were measured 3 times.

Results and Discussion

Characteristics of the GBP-Based Glucose Assay. The engineered glucose binding protein described here has a single cysteine mutation at 255 where a polarity sensitive probe acrylodan is covalently attached. The labeled acrylodan emits strong green fluorescence (510 nm) when excited with violet light (380 nm). In the presence of glucose, the fluorescence intensity of acrylodan decreases with glucose concentration. A typical calibration curve of the glucose biosensor is shown in Figure 2. It can be seen that the calibration curve is almost linear at low glucose concentrations but gradually saturates at higher glucose concentration. The thick black line with circles shows the average relative error of the biosensor at different glucose concentrations. The average relative error is defined as

$$\text{error (\%)} = \frac{\Delta G}{\overline{G}} \times 100 \qquad (1)$$

where ΔG is the standard deviation of the measured glucose concentrations, and $\overline{G}$ is the average of the measured glucose concentrations. Obviously, the average relative error reaches its minimum, which is 2.1%, at glucose concentration of 2.0 μM. If the slope of the calibration curve in Figure 2 is defined as the sensitivity of the assay, the standard deviation of the measured glucose concentrations in eq 1 is then equal to

$$\Delta G = \frac{\Delta S}{m} \qquad (2)$$

where ΔS is the standard deviation of the measured signal changes, and m is the sensitivity of the assay at measured glucose concentration. Substitution of eq 2 into eq 1 gives

$$\text{error (\%)} = \frac{\Delta S}{m\overline{G}} \times 100 \qquad (3)$$

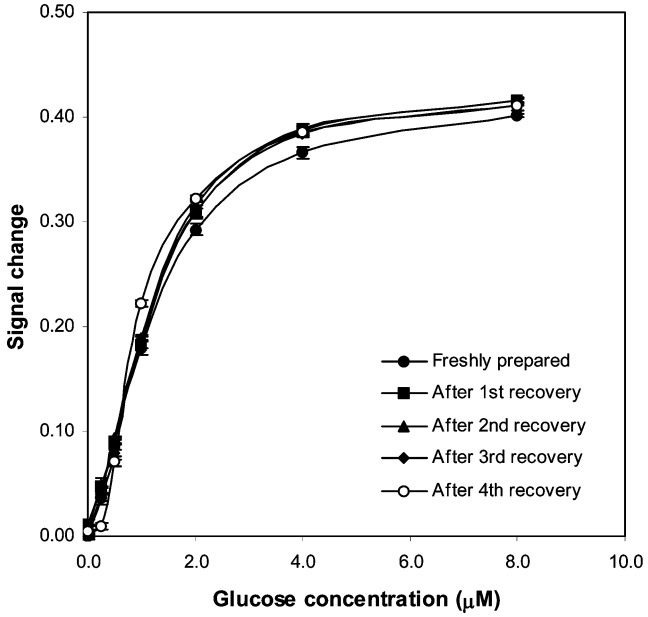

Figure 3. Reusability of the labeled glucose binding protein.

It can be seen that the average relative error of the measured glucose concentrations is proportional to the standard deviation of the measured signal changes and inversely proportional to the measured glucose concentration and the sensitivity of the assay at that concentration. At low glucose concentrations, the average relative error is higher because $\overline{G}$ is small although the sensitivity of the assay, m, is high. On the other hand, the average relative error is also higher at high glucose concentrations because of low sensitivity. At medium glucose concentrations, the two factors offset somewhat and the average relative error of the measured glucose concentrations is lower. The thick black line without symbols gives the average relative error of the measured glucose concentrations caused by 1% standard deviation of fluorescence intensity measurements. It can be seen that 1% intensity measurement error can cause a relative error of 10% or higher for glucose concentrations. This means that it is very critical to accurately measure the fluorescence intensity. One way to effectively decrease the errors is to read the fluorescence intensity many times and then average the data (*38*). Accordingly, averaging reduces the lower limit of detection (*45*) up to 5 times depending on how many measurements are averaged.

As shown in Figure 2, the biosensor has micromolar sensitivity for glucose. Although the detection range can be broadened by increasing the concentration of the GBP as previously described (*34*−*38*), it cannot be easily extended to measure millimolar glucose solely by increasing the GBP concentration because of the concentration limit. Therefore, physiological concentrations of glucose, which are in the millimolar range, require a dilution step prior to measurement with this biosensor. Alternatively, sampling techniques that inherently dilutes the sample such as microdialysis and iontophoresis are especially applicable. In clinical diagnostics applications, these techniques generally sample the interstitial fluid rather than venous blood. Although the glucose concentration in interstitial fluid is similar to blood, when extracted by iontophoresis the concentration is reduced to 0−30 μM (*20*). Note that these concentrations fit the responsive range of the glucose sensor discussed here. In the case of microdialysis, the concentration of glucose in the dialysate depends on the dimensions of the microdialysis membrane, properties of the membrane material, the perfusion flow rate and the temperature. However, in general, practical

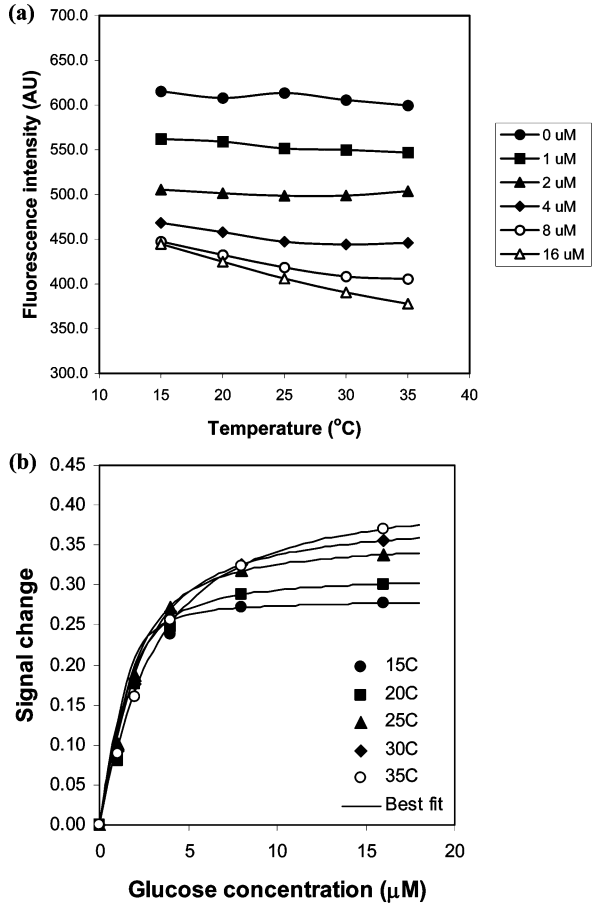

Figure 4. Change of the fluorescence intensity with temperature at different glucose concentrations (a) and the best fits to the calibration data at different temperatures (b).

considerations give rise to submillimolar concentrations of glucose in the dialysate. For dialysates at such low glucose levels, the conventional glucose oxidase-based methods are more difficult to implement as these concentrations approach the limit of detection. It is clear that, in contrast, GBP can be used for glucose measurements in these submillimolar concentrations. Nevertheless, some preliminary measurements may be required to determine the proper dilution of the samples and appropriate calculations to determine the concentration of glucose in the original sample.

To check if the labeled GBP is reusable, used GBP was recovered after the assay and its reusability was studied. After the assay, the GBP was no longer responsive to glucose because of the bound glucose. To remove the bound glucose, used GBP solution was injected into a dialysis bag, which was then dialyzed in PBS buffer at 4 °C for 2 h. After that, the PBS buffer was replaced with fresh buffer and the GBP solution was dialyzed for another 2 h. After that, 99.99% of the bound glucose was removed from the GBP solution. The GBP solution could then be transferred from the dialysis bag to a sterile plastic tube for tests. Results show that the calibration curves do not change significantly after several recoveries (Figure 3). These experiments prove that should the protein sensor be immobilized on a solid surface, it will result in a reversible and reusable sensor.

For any analytical method, it is very important to study what factors affect the measurements and, thus, should be controlled or set. For the GBP glucose biosensor, the temperature is a very important factor because it affects both the fluorescence as well as the protein structural dynamics. Figure 4a shows the changes in fluorescence intensity of the labeled GBP with temperature at different glucose concentrations. As expected, the fluorescence intensity of the labeled protein decreases with temperature. The data in Figure 4a can be re-plotted to get Figure 4b. The apparent binding constants could be calculated by fitting the experimental results to the binding isotherm:

$$\Delta F = \frac{\Delta F_{\max} G}{K_d + G} \tag{4}$$

where ΔF is the normalized signal change at any glucose concentration, $\Delta F_{\max}$ is the normalized signal change at saturating glucose concentration, K_d is the apparent binding constant, and G is the glucose concentration in free state. The symbols in Figure 4b represent the experimental data and the lines are the best nonlinear fit to eq 4. The results for $\Delta F_{\max}$ and K_d at different temperatures are listed in Table 1. Further analysis of this data was not done to determine the contributions of nonradiative deactivation of the fluorophore and fluctuations in the protein structure to the observed decrease in intensity. Nevertheless, it is clear that temperature control is absolutely imperative in using this biosensor.

Figure 5 shows the calibration curves for glucose and five other sugars. It can be seen that in addition to glucose the GBP biosensor also responds to galactose although to a lesser extent. The GBP biosensor is significantly less sensitive to other sugars, although they show some minor effects at these concentrations. It should be noted that culture media, blood and interstitial fluid usually have negligible amounts of these other sugars in comparison to glucose. Exceptions are patients with galactosemia and some newborns, whose blood contains elevated galactose (6−10 mg/dL).

Microdialysis. Figure 6a shows the relationship between the dialysis efficiency (E) and the perfusion rate at two different temperatures. The dialysis efficiency is defined as

$$E = \frac{C}{C_b} \times 100\% \tag{5}$$

where C is the glucose concentration in the dialysate, and C_b is the glucose concentration in the media. It can be seen that the glucose concentration in the media has no effect on the dialysis efficiency but temperature and perfusion flow rate have a great effect.

Suppose that the glucose concentration in the bioreactor is well-mixed and the perfusion buffer in the dialysis probe is a plug flow, then the mass balance for the glucose diffusing across the probe membrane yields the flowing equation:

$$\upsilon dC = k2\pi r dx(C_b - C) \tag{6}$$

where C is the glucose concentration in the perfusion buffer at position x, k is mass transfer coefficient, r is the radius of the dialysis probe, and υ is the perfusion rate. Integration of eq 6 gives

$$\ln(1 - E) = -\frac{2\pi r k L}{\upsilon} \tag{7}$$

where L is the length of the dialysis probe. Figure 6b shows that the glucose concentration in the dialysate agrees very well with eq 7.

Figure 7 shows the delay time and dialysis efficiency at different perfusion rates. The delay time is defined as the time needed for the perfusion buffer to flow from the dialysis probe to the collection tube. Both delay time and dialysis efficiency change inversely with the perfusion rate. Because the GBP

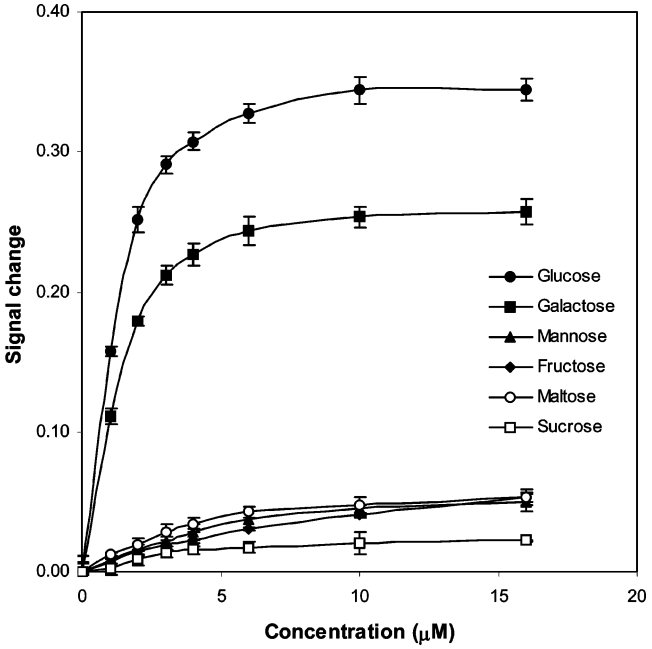

Figure 5. Sensitivity of the labeled GBP to different sugars.

Table 1. Best Nonlinear Fit Results of Maximum Signal Changes (ΔF_{max}) and Apparent Binding Constants (K_d) at Different Temperatures

temp, °C	ΔF_{max}	K_d, μM
15	0.282 ± 0.002	0.25 ± 0.06
20	0.313 ± 0.002	0.56 ± 0.07
25	0.357 ± 0.001	0.82 ± 0.04
30	0.385 ± 0.002	1.20 ± 0.06
35	0.421 ± 0.002	1.99 ± 0.06

biosensor is sensitive at very low concentrations, high dialysis efficiency (i.e., approaching 100%) is not required. In fact, at a limit of detection (LOD) of 0.04 μM (*38*), a dialysis efficiency of 0.02% will provide glucose concentrations that are about 100X the LOD. The commercially available microdialysis system used in this study even at the fastest perfusion rate is still too efficient. Thus, future work will require adjustment of the microdialysis conditions to decrease efficiency by either decreasing the dimensions of the probe or fabricating new material for the microdialysis membrane. Nevertheless, in the mammalian cell culture experiments, though not ideal, a perfusion rate of 10 μL/min was selected. Accordingly, collection of the dialysate and further dilution to within the sensitivity range of the GBP sensor was required. Even at this rate, the delay time is less than 1 min. Other glucose analysis methods that require high dialysis efficiencies are reported to have a lag time of 30−35 min. Thus, with further optimization our method can approach real time monitoring of glucose.

At 10 μL/min perfusion rate, the dialysis efficiency is about 5%. Thus, if 100 μL of dialysate is collected each time, the glucose concentration in the bioreactor decreases by only 0.14% because of the dialysis. Therefore, the effect of dialysis itself on the glucose concentration in the bioreactor is negligible.

Mammalian Cell Culture. A SP2/0 based myeloma/mouse hybridoma cell line was grown in the bioreactor shown in Figure 1 at 37 °C and 100 rpm. The pH and dissolved oxygen concentration were monitored by disposable sensing patches. The cell density reached its maximum at about 100 h and then declined rapidly (Figure 8). As the cells grew and consumed more oxygen before reaching the highest cell density, the dissolved oxygen gradually declined from 100% air saturation to 76% and then recovered rapidly to 100% at the end of the

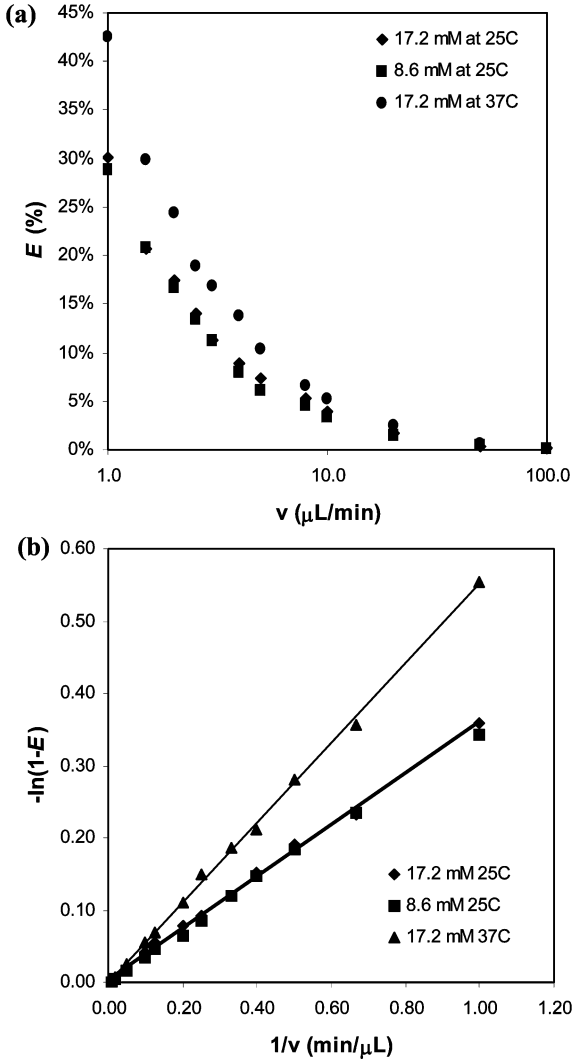

Figure 6. Relation between dialysis efficiency and bulk glucose concentration, perfusion rate, and temperature.

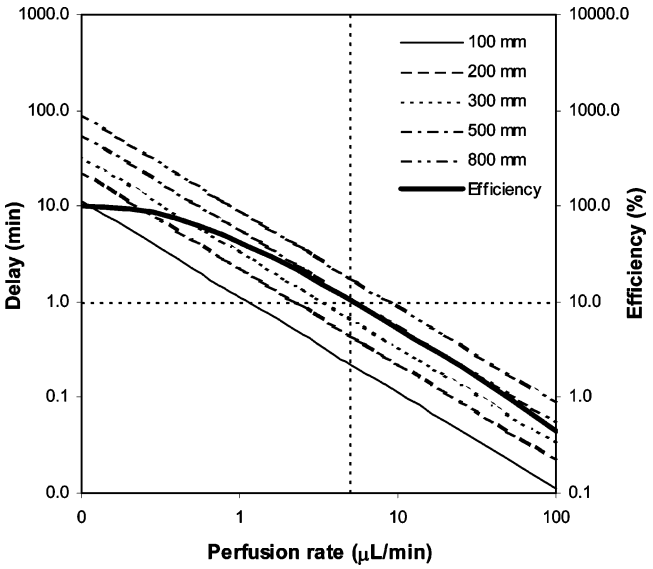

Figure 7. Delay time and dialysis efficiency at different perfusion rates.

culture process due to the death of the cells. As the seed culture was originally maintained in 5% CO_2, pH quickly increased at the beginning of the culture process due to the loss of the dissolved CO_2 from the culture.

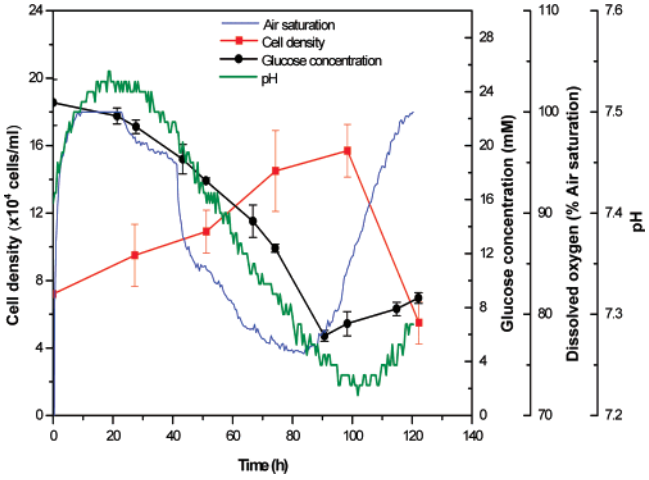

Figure 8. Glucose concentration, DO, pH, and cell density profiles in mammalian cell culture.

Although the glucose concentration in the dialysate agrees very well with eq 5, the mass transfer coefficient k can be affected by many factors such as temperature, the viscosity of the media, stirring speed, etc. Additionally, the presence of cells or macromolecules in the media may also affect the dialysis efficiency as some of the pores in the dialysis probe may be blocked by the cells or macromolecules. In this study, the beginning dialysis efficiency was determined by the glucose concentrations in the beginning culture and the first dialysis sample taken immediately after the start of the cell culture. The ending dialysis efficiency was determined by the glucose concentrations in the final culture and the last dialysis sample taken immediately before the end of the culture. The beginning dialysis efficiency is higher than the ending dialysis efficiency, showing that some of the pores were blocked during the cell culture. Assuming a linear decline for the dialysis efficiency, the glucose concentrations in the culture were calculated and shown in Figure 8. Results show that the glucose concentration decreased as the cells grew and consumed glucose. At the late stage of the cell culture, the glucose concentration gradually increased. As the cells begin to lose viability, they undergo lysis thereby discharging their contents into the surrounding medium.

Conclusion

We have shown that the fluorescent GBP is a potential sensor for real-time monitoring of glucose in cell culture using microdialysis. The submicromolar limit of detection of GBP allows for minimal microdialysis efficiency. Thus, the fast perfusion flow rates utilized in this work resulted in time lags of about 1 min. Less sensitive sensors like those using glucose oxidase require slower flow rates, resulting in much longer time lags. Nonetheless, flow rates beyond the capability of the microdialysis device used here (>100 μL/min) should provide glucose levels well above the limit of detection of GBP. Thus, further work is needed to customize either the dimensions of the microdialysis probe or the material of the semipermeable membrane to allow for lower glucose concentrations in the dialysate while approaching real-time monitoring. Additionally, material that will resist cell-adhesion and biofouling will be investigated.

Acknowledgment

The authors acknowledge the support of the National Institutes of Health through grants DK062990 and DK072465 and the U.S. Army Medical Research and Materiel Command through grant W81XWH-04-1-0781. The *E. coli* NM303 was from cultures originally provided by Dr. W. Boos, University Konstanz, Germany.

References and Notes

(1) Campuzano, S.; Gálvez, R.; Pedrero, M.; Manuel de Villena, F J.; Pingarrón, J M. Preparation, Characterization and Application of Alkanethiol Self-Assembled Monolayers Modified with Tetrathiafulvalene and Glucose Oxidase at a Gold Disk Electrode. *J. Electroanal. Chem.* **2002**, *526*, 92−100.

(2) Chen, T.; Friedman, K. A.; Lei, I.; Heller, A. In Situ Assembled Mass-Transport Controlling Micromembranes and Their Application in Implanted Amperometric Glucose Sensors. *Anal. Chem.* **2000**, *72*, 3757−3763.

(3) Gouda, M. D.; Kumar, M. A.; Thakur, M. S.; Karanth, N. G. Enhancement of Operational Stability of an Enzyme Biosensor for Glucose and Sucrose Using Protein Based Stablizing Agents. *Biosens. Bioelectron.* **2002**, *7*, 503−507.

(4) Haouz, A.; Stieg, S. Continuous Monitoring of D-Glucose and L-lactate by Flow Injection Analysis. *Enzyme Microb. Technol.* **2002**, *30*, 129−133.

(5) Miscoria, S. A.; Desbrieres, J.; Barrera, G. D.; Labbé, P.; Rivas, G. A. Glucose Biosensor Based on the Layer-by-Layer Self-Assembling of Glucose Oxidase and Chitosan Derivatives on a Thiolated Gold Surface. *Anal. Chim. Acta* **2006**, *578* (2), 137−144.

(6) Mignani, A.; Scavetta, E.; Tonelli, D. Electrodeposited Glucose Oxidase/Anionic Clay for Glucose Biosensors Design. *Anal. Chim. Acta* **2006**, *577* (1), 98−106.

(7) Endo, H.; Yonemori, Y.; Musiya, K.; Maita, M.; Shibuya, T.; Ren, H.; Hayashi, T.; Mitsubayashi, K. A Needle-Type Optical Enzyme Sensor System for Determining Glucose Levels in Fish Blood. *Anal. Chim. Acta* **2006**, *573*−*574*, 117−124.

(8) Kang, X.; Mai, Z.; Zou, X.; Cai, P.; Mo, J. A Novel Glucose Biosensor Based on Immobilization of Glucose Oxidase in Chitosan on a Glassy Carbon Electrode Modified with Gold-Platinum Alloy Nanoparticles/Multiwall Carbon Nanotubes. *Anal. Biochem.* **2007**, *369* (1), 71−79.

(9) Dai, Z.; Fang, M.; Bao, J.; Wang, H.; Lu, T. An Amperometric Glucose Biosensor Constructed by Immobilizing Glucose Oxidase on Titanium-Containing Mesoporous Composite Material of no. 41 Modified Screen-Printed Electrodes. *Anal Chim Acta* **2007**, *591* (2), 195−199.

(10) Ekanayake, E. M.; Preethichandra, D. M.; Kaneto, K. Polypyrrole Nanotube Array Sensor for Enhanced Adsorption of Glucose Oxidase in Glucose Biosensors. *Biosens. Bioelectron.* **2007**, *23* (1), 107−113.

(11) Henninger, N.; Woderer, S.; Kloetzer, H. M.; Staib, A.; Gillen, R.; Li, L.; Yu, X.; Gretz, N.; Kraenzlin, B.; Pill, J. Tissue Response to Subcutaneous Implantation of Glucose-Oxidase-Based Glucose Sensors in Rats. *Biosens. Bioelectron.* **2007**, *23* (1), 26−34.

(12) Ballerstadt, R.; Schultz, J. S. A Fluorescence Affinity Hollow Fiber Sensor for Continuous Transdermal Glucose Monitoring. *Anal. Chem.* **2000**, *72*, 4185−4192.

(13) Meadows, D. L.; Schultz, J. S. Design, Manufacture and Characterization of an Optical Fiber Glucose Affinity Sensor Based on an Homogeneous Fluorescence Energy Transfer Assay System. *Anal. Chim. Acta* **1993**, *280*, 21−30.

(14) McCartney, L. J.; Pickup, J. C.; Rolinski, O. J.; Birch, D. J. S. Near-Infrared Fluorescence Lifetime Assay for Serum Glucose Based on Allophycocyanin-Labeled Concanavalin A. *Anal. Biochem.* **2001**, *292* (2), 216−221.

(15) Russell, R. J.; Pishko, M. V. A Fluorescence-Based Glucose Biosensor Using Concanavalin A and Dextran Encapsulated in a Poly(ethylene glycol) Hydrogel. *Anal. Chem.* **1999**, *71*, 3126−3132.

(16) D'Auria, S.; Di Cesare, N.; Gryczniski, Z.; Gryczniski, I.; Rossi, M.; Lakowicz, J. R. A Thermophilic Apo-Glucose Dehydrogenase as Non-Consuming Glucose Sensor. *Biochem. Biophys. Res. Commun.* **2000**, *274*, 727−731.

(17) D'Auria, S.; Herman, P.; Rossi, M.; Lakowicz, J. R. The Fluorescence Emission of Apo-Glucose Oxidase from Aspergillus Niger as Probe to Estimate Glucose Concentrations. *Biochem. Biophys. Res. Commun.* **1999**, *263*, 550−553.

(18) D'Auria, S.; Lakowicz, J. R. Enzyme Fluorescence as a Sensing Tool: New Perspectives in Biotechnology. *Curr. Opin. Biotechnol.* **2001**, *12*, 99−104.
(19) Heinemann, L. Continuous Glucose Monitoring by Means of the Microdialysis Technique: Underlying Fundermental Aspects. *Diabetes Technol. Ther.* **2003**, *5* (4), 545−561.
(20) Sieg, A.; Guy, R. H.; Delgado-Charro, M. B. Noninvasive Glucose Monitoring by Reverse Iontophoresis in Vivo: Application of the Internal Standard Concept. *Clin. Chem.* **2004**, *50* (8), 1383−1390.
(21) Gebhart, S.; Faupel, M. D.; Fowler, R.; Kapsner, C.; Lincoln, D.; Mcgee, V.; Pasqua, J.; Steed, L.; Steed, M.; Wangsness, M.; Xu, F.; Vanstory, M.; Burdick, J.; Chase, B. A.; Faupel, M.; Schultz, B.; Gebhart, S. Real-Time Glucose Sensing using Transdermal Fluid under Continuous Vacuum Pressure in Children with Type 1 Diabetes. *Diabetes Tech. Therap.* **2003**, *5*, 159−166.
(22) Burdick, J.; Chase, B. A.; Faupel, M.; Schultz, B.; Gebhart, S. Real-Time Glucose Sensing using Transdermal Fluid under Continuous Vacuum Pressure in Children with Type 1 Diabetes. *Diabetes Tech. Therap.* **2005**, *7*, 448−455.
(23) Dattelbaum, J. D.; Lakowicz, J. R. Optical Determination of Glutamine Using a Genetically Engineered Protein. *Anal. Biochem.* **2001**, *291*, 89−95.
(24) Gilardi, G.; Mei, G.; Rosato, N.; Agro, A. F.; Cass, A. E. G. Spectroscopic Properties of an Engineered Maltose Binding Protein. *Protein Eng.* **1997**, *10* (5), 479−486.
(25) Gilardi, G.; Zhou, L. Q.; Hibbert, L.; Cass, A. E. G. Engineering the Maltose Binding Protein for Reagentless Fluorescence Sensing. *Anal. Chem.* **1994**, *66*, 3840−3847.
(26) Kubo, I. Potentiometric Phosphate-Sensing System Utilizing Phosphate-Binding Protein. *Anal. Bioanal. Chem.* **2002**, *372*, 273−275.
(27) Marvin, J. S.; Hellinga, H. W. Engineering Biosensors by Introducing Fluorescent Allosteric Signal Transducers: Construction of a Novel Glucose Sensor. *J. Am. Chem. Soc.* **1998**, *120*, 7−11.
(28) Naal, Z.; Park, J. H.; Bernhard, S.; Shapleigh, J. P.; Batt, C. A.; Abruna, H. D. Amperometric TNT Biosensor Based on the Oriented Immobilization of a Nitroreductase Maltose Binding Protein Fusion. *Anal. Chem.* **2002**, *74*, 140−148.
(29) Salins, L. L. E.; Ware, R. A.; Ensor, C. M.; Daunert, S. A Novel Reagentless Sensing System for Measuring Glucose Based on the Galactose/Glucose-Binding Protein. *Anal. Chem.* **2001**, *294*, 19−26.
(30) Tolosa, L.; Gryczynski, I.; Eichhorn, L. R.; Dattelbaum, J. D.; Castellano, F. N.; Rao, G.; Lakowicz, J. R. Glucose Sensor for Low-Cost Lifetime Based Sensing Using a Genetically Engineered Protein. *Anal. Biochem.* **1999**, *267*, 114−120.
(31) Tian, Y.; Cuneo, M. J.; Changela, A.; Hocker, B.; Beese, L. S.; Hellinga, H. W. Structure-Based Design of Robust Glucose Biosensors using a Thermotoga maritima Periplasmic Glucose-Binding Protein. *Protein Sci.* **2007**, *16* (10), 2240−2250.
(32) Cuneo, M. J.; Changela, A.; Warren, J. J.; Beese, L. S.; Hellinga, H. W. The Crystal Structure of a Thermophilic Glucose Binding Protein Reveals Adaptations That Interconvert Mono and Disaccharide Binding Sites. *J. Mol. Biol.* **2006**, *362* (2), 259−270.
(33) Ye, K.; Schultz, J. S. Genetic Engineering of an Allosterically Based Glucose Indicator Protein for Continuous Glucose Monitoring by Fluorescence Resonance Energy Transfer. *Anal. Chem.* **2003**, *75*, 3451−3459.
(34) Ge, X.; Tolosa, L.; Simpson, J.; Rao, G. Genetically Engineered Binding Proteins as biosensors for Fermentation and Cell Culture. *Biotechnol. Bioeng.* **2003**, *84* (6), 723−731.
(35) Tolosa, L.; Ge, X.; Rao, G. Reagentless Optical Sensing of Glutamine using a Dual-Emitting Glutamine-Binding Protein. *Anal. Biochem.* **2003**, *314* (2), 199−205.
(36) Ge, X. Development of novel optical sensors for fermentation and cell culture. Ph.D. dissertation. University of Maryland, Baltimore County, 2004.
(37) Ge, X.; Tolosa, L.; Rao, G. Dual-labeled Glucose Binding Protein for Ratiometric Measurements of Glucose. *Anal. Chem.* **2004**, *76* (5), 1403−1410.
(38) Ge, X.; Lam, H.; Modi, S. J.; LaCourse, W. R.; Rao, G.; Tolosa, L. Comparing the Performance of the Optical Glucose Assay Based on the Glucose Binding Protein with High Performance Anion-exchange Chromatography with Pulsed Electrochemical Detection: Efforts to Design a Low-Cost Point-of-Care Glucose Sensor. *J. Diabetes Sci. Technol.* **2007**.
(39) Quiocho, F. A. Atomic Structure of Periplasmic Binding Proteins and the High-Affinity Active Transport Systems in Bacteria. *Philos. Trans. R. Soc. London, Ser. B* **1990**, *326*, 341−351.
(40) Hsiao, C. D.; Sun, Y. J.; Rose, J.; Wang, B. C. The Crystal Structure of Glutamine-binding Protein from Escherichia coli. *J. Mol. Biol.* **1996**, *262*, 225−242.
(41) Sun, Y. J.; Rose, J.; Wang, B. C.; Hsiao, C. D. The Structure of Glutamine-binding Protein Complexed with Glutamine at 1.94 A Resolution: Comparisons with other Amino Acid Binding Proteins. *J. Mol. Biol.* **1998**, *278*, 219−229.
(42) Hellinga, H. W.; Marvin, J. S. Protein Engineering and the Development of Generic Biosensors. *TIBTECH* **1998**, *16*, 183−189.
(43) Haughland, R. P. *Handbook of Fluorescent Probes and Research Chemicals*; Molecular Probes, Inc.: Eugene, OR, 1996.
(44) Ge, X.; Hanson, M.; Kostov, Y.; Moreira, A. R.; Rao, G. Validation of an optical sensor-based high-throughput bioreactor system for mammalian cell culture. *J. Biotechnol.* **2006**, *122* (3), 293−306.
(45) Long, G. L.; Winefordner, J. D. Limit of detection − a closer look at the IUPAC definition. *Anal. Chem.* **1983**, *55* (7), 712A−724A.

Received October 30, 2007. Accepted March 5, 2008.

BP070411K